Astronomy Letters, 2014, Vol. 40, No. 11, p. 667–690. Translated from Pis'ma v Astronomicheskij Zhurnal.

Measurements of the Cosmic X-ray Background of the Universe and the MVN Experiment

M. G. Revnivtsev[*1]

[1] *Space Research Institute of RAS (IKI), Moscow, Russia*

Received May 22, 2014

Abstract — The paper describes previous studies of the cosmic X-ray background (CXB) of the Universe in the energy range 1-100 keV and outline prospects for its investigation with the help of MVN (Monitor Vsego Neba) experiment. The nature of the CXB and its use for studying the cosmological evolution of black holes are briefly discussed. The bulk of the paper is devoted to the methods of CXB measurements, from the first pioneering rocket and balloon-borne experiments to the measurements made with latest-generation orbital X-ray observatories. Particular attention is given to the problems of allowance for the contribution of background events to the measurements with X-ray and hard X-ray instruments.

arXiv:1410.3284v1 [astro-ph.HE] 13 Oct 2014

1. INTRODUCTION

The background emission of the sky in the X-ray energy range (1-10 keV) is one of the first discoveries in X-ray astronomy. The very first experiment whose goal was the search for a non-solar X-ray emission discovered two entirely new phenomena: the brightest source in the X-ray sky, Scorpius X-1 (a close binary star system with a neutron star), and a nearly isotropic sky emission, the cosmic X-ray background of the Universe (Giacconi et al., 1962). At energies below 1-2 keV, the background emission of the sky is significantly anisotropic and has a different nature: the hot-gas emission in our Galaxy (see, e.g., the review by McCammon & Sanders 1990.

The first experiments in X-ray astronomy were carried out with high-altitude rockets capable of bringing the recording equipment to altitudes higher than 100 km (the experiments of the group from the US Naval Research Laboratory, Friedman et al., are among the best-known ones; see the review by Mandelshtam & Efremov (1957)), on which the X- ray absorption by the residual atmosphere is already insignificant. The Sun was the object of observations in the first experiments in the X-ray energy range. The X-ray flux from the sky in these experiments was observed with Geiger (gas) counters. The Suns observations did not require a high-sensitivity of instruments because of its considerable flux. Therefore, the X-ray flux from the Sun was generally measured by integrating the total signal over certain time intervals; no filtering of background events was performed.

The main problem of recording the X-ray emission of the sky is the background count rate that arises in the detectors of this energy range even in the absence of its real illumination by X-ray photons. Charged cosmic-ray particles, mostly protons and electrons, are the source of this background count rate. Great progress in the sensitivity of gas counters to (relatively) faint X-ray sources was achieved in 1962, when an active anticoincidence shield was used to separate the events due to the passage of charged particles from the events related to the absorption of X-ray photons; it allowed the background count rate to be reduced by more than a factor of 100. This led both to the discovery of discrete X-ray sources in the sky and to the detection of a nearly isotropic background emission.

The cosmic X-ray background was detected in the original experiment of the ASE (American Science and Engineering) group as a lower level of the ener- getic particle count rate observed irrespective of the direction of the instruments field of view. The authors of the work provided arguments that these particles were not charged ones but were X-ray photons (Giacconi et al., 1962). The cosmic X-ray background (CXB) has since been one of the main goals of the operation of any orbital X-ray astrophysical observatory. A review of the results of early experiments can be found in Horstman et al. (1975); Tanaka & Bleeker (1977); Boldt (1987).

2. THE COSMIC X-RAY BACKGROUND OF THE UNIVERSE

The first measurements of the CXB spectrum were made by means of short (with an effective exposure time of only ∼300 s) rocket experiments in the energy range 1-6 keV and observations from stratospheric balloons at energies above 20 keV. In these energy

[*] e-mail: revnivtsev@hea.iki.rssi.ru

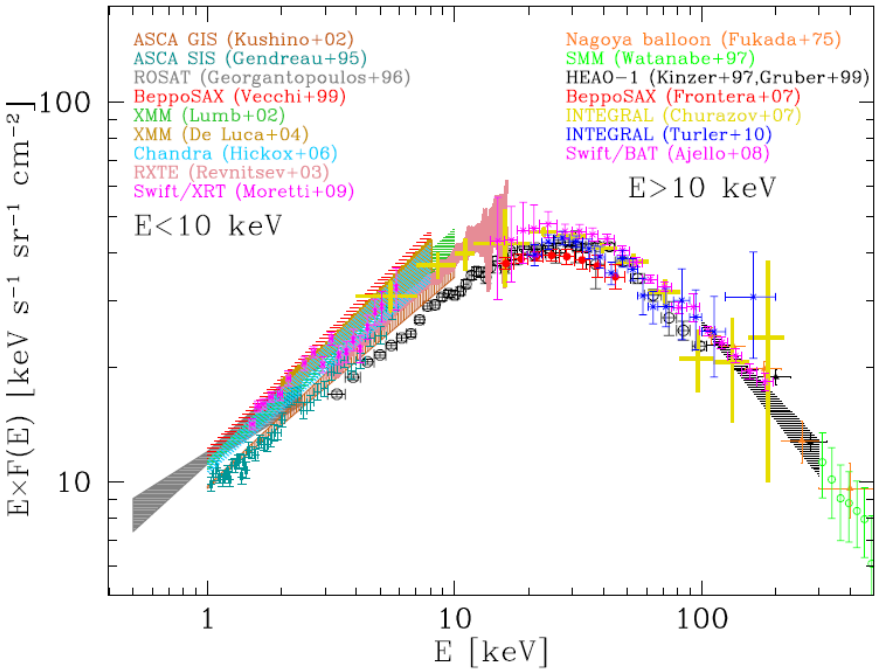

Fig. 1. Energy spectrum of the CXB of the Universe from the measurements of several orbital observatories. The maximum energy in the CXB is seen to be concentrated in the range 5-100 keV. The shape of the CXB spectrum can be satisfactorily described by a power law $dN/dE \propto E^{-\Gamma}$ with photon index $\Gamma \approx 1.4$ at energies below 10 keV and a photon index $\Gamma \approx 2.5$ at energies above 50 keV (from Gilli 2013).

ranges, the CXB spectrum was individually defined as a power-law dependence of the photon number density on energy, $dN/dE \propto E^{-\Gamma}$. However, it turned out that the measurements systematically showed a difference in the slopes of the power-law spectra at energies below and above 10 keV ($\Gamma \approx 1.4$ below 10 keV and $\Gamma \approx 2.5$ above 20-30 keV). Subsequently, higher-quality measurements of the CXB spectrum showed that its hardness actually decreased in the energy range 20-30 keV and, on the whole, the CXB spectrum in the range 1-60 keV could be described by the model of emission from an optically thin plasma with a temperature of 40 keV. As a result of these measurements, it was hypothesized that the CXB was the result of emission from a hot intergalactic plasma with a temperature of 40 keV (see, e.g., the reasoning in the early works of Felten & Morrison 1966; Silk 1970).

Measurements of the shape of the cosmic microwave background (CMB) spectrum impose the most stringent constraints on the existence of such a hot intergalactic plasma. In the presence of a hot plasma on the line of sight, the CMB photons must undergo Compton scattering and gain energy from energetic electrons in the intergalactic plasma. As a result, the so-called y-distortion of the CMB spectrum, the Sunyaev-Zeldovich effect, must be produced (see, e.g., Sunyaev & Zeldovich 1970).

The measurements made by the COBE orbital observatory showed the CMB spectrum to be an essentially Planckian spectrum of a perfect blackbody with the possibilities of a deviation for the parameter y by no more than $y < 2.5 \times 10^{-5}$ (Mather et al., 1994; Wright et al., 1994). This means that the vast bulk of the CXB flux cannot arise in the hot intergalactic gas but must be produced by the total emission from a large number of discrete sources.

The first direct measurements of a significant contribution of the flux from a large number of discrete sources to the CXB became possible after the advent of X-ray telescopes with grazing-incidence mirrors (first proposed by Giacconi & Rossi 1960). The first astrophysical X-ray telescope onboard the HEAO2/Einstein orbital observatory (1978-1981) allowed a record (at that time) sensitivity of 1.3×10^{-14} erg s^{-12} cm^{-2} in the energy range 1-3 keV to be achieved. At this sensitivity level, the surface density of detected sources was already $\sim$20 sources deg^{-2} (Giacconi et al., 1979).

At present, using the latest-generation telescopes of the Chandra and XMM-Newton observatories, it is possible to resolve more than 80-90% of the CXB flux at energies 1-2 keV into the contribution of point sources with a surface density up to 10 000 per square

degree (see Moretti et al. 2003; Hickox & Markevitch 2006, 2007).

The overwhelming majority of the sources that contribute to the observed CXB surface brightness are active galactic nuclei (AGNs), accreting super- massive black holes, at various distances from us Setti & Woltjer (1989). It is estimated that the emission from ordinary galaxies and galaxy clusters must contribute at energies below 2-5 keV. Since the X-ray emission in AGNs arises from the accretion of matter onto supermassive black holes, the CXB surface brightness is actually an overall measure of the growth of all supermassive black holes in the history of the Universe (Soltan, 1982; Fabian & Iwasawa, 1999; Gilli et al., 2007; Ueda et al., 2014).

Combining the CXB surface brightness measurements with the studies of the counts of individual classes of sources in various deep sky surveys allows the long-term evolution of the growth of supermassive black holes to be studied.

A study of the latter showed that they could be observationally separated into several large classes. In the so-called unification model (Urry & Padovani, 1995), the observational manifestations of AGNs in a broad wavelength band (from the radio and infrared to the X-ray range) depend on the AGN inclination to an observers line of sight. The emission from the central region of AGNs observed at an angle close to 90 passes through a dense dusty torus and is absorbed up to the hard X-ray band, being reprocessed into the infrared (the so-called type 2 AGN, Seyfert 2, absorbed AGNs). Manifestations of an accretion disk in the ultraviolet and the soft X-ray band are clearly seen in the spectra of AGNs observed at small angles to the line of sight (the so-called type 1 AGNs, Seyfert 1). AGNs observed along the direction of the relativistic jet ejection from the central black hole are recorded as blazars in a very wide wavelength range, from the radio to ultrahigh-energy gamma rays (see, e.g., the review by Böttcher 2007).

Simulations of the properties of a population of AGNs at various redshifts (see, e.g., Gilli et al. 2007; Sazonov et al. 2008; Ueda et al. 2014) show that the AGNs surrounded by dust clouds with a column density on the line of sight $\log N_H L > 23$ cm^{-2} make a large contribution to the CXB surface brightness at energies above 5-7 keV (see Fig. 2).

The contribution of such AGNs and, hence, the total density of black holes in the Universe can be estimated accurately only by using information about the shape of the CXB spectrum at energies above 5-7 keV.

An important feature of the CXB is that its surface brightness contains the emission from all arbitrarily faint objects in the Universe, even those that are virtually impossible to observe separately with X-ray telescopes because of their (telescopes) finite sensitivity.

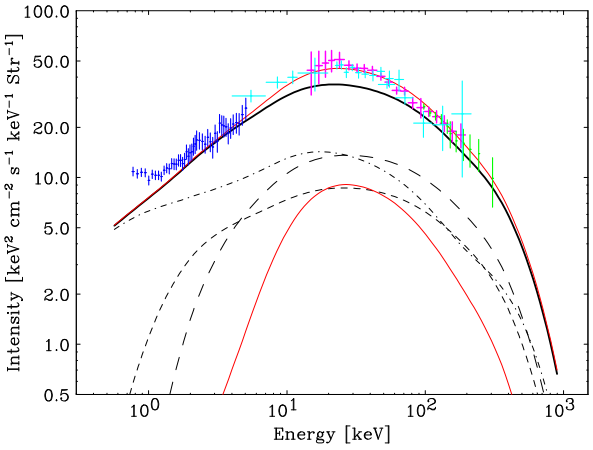

Fig. 2. Spectrum of the CXB of the Universe and its description by the contribution of AGNs with various degrees of absorption. The upper thin solid curve indicates the complete model of emission from the sum of AGNs with absorption on the line of sight from a column density $\log N_H L < 22$ cm^{-2} to $\log N_H L \sim 26$ cm^{-2}. The lower thin solid curve indicates the contribution of the so-called Compton-thick AGNs with a column density on the line of sight $\log N_H L = 24 - 26$ cm^{-2} (from Ueda et al. 2014).

This opens the possibility of measuring the total (including the contribution of arbitrarily faint objects) emissivity of the Universe. In the nearby Universe (at distances up to 70-100 Mpc from us), such a measurement can be made by using the property of matter clumpiness on these spatial scales. Over the evolution time of the Universe, the mutual attraction of matter (including dark matter) gave rise to significant density inhomogeneities with a contrast of more than unity. Since X-ray bright objects (AGNs, X-ray binary systems, etc.) must trace the distribution of baryonic matter, the X-ray volume emissivity of the Universe must vary in space.

In observations of the X-ray sky, such variations in the X-ray volume emissivity of the Universe must be observed as increases and decreases of the CXB surface brightness in different directions: the distribution of objects in the distant Universe will be averaged over the directions, while the large inhomogeneities in matter density at distances of 50-100 Mpc must manifest themselves. If the distribution of matter (for example, galaxies) is known, then the amplitude of the CXB surface brightness variations can be recalculated to the total X-ray luminosity per unit volume of the nearby Universe.

The first attempts at such measurements were made using the sky survey with the A2 instrument onboard the HEAO1 observatory (Jahoda et al., 1991; Boldt,

1992; Miyaji et al., 1994; Scharf et al., 2000). The RXTE sky survey was used for the same purpose in Revnivtsev et al. (2008). New measurements of the CXB surface brightness and its distribution over the sky with accuracies better than 1-2% are needed to accurately measure the emissivity of the nearby Universe and to estimate the contribution of the emission from faint sources to it.

3. THE PROBLEMS OF CXB MEASUREMENTS

The problem of CXB measurements can be separated into several components:

1. The problem of an accurate energy calibration of the instrument is related to the fact that the CXB surface brightness decreases rapidly with increasing photon energy. Therefore, even small errors in calibrating the energy scale of the detector will lead to significant deviations of the measured CXB surface brightness from its true value. This question is considered in more detail in Section 4.

2. The problem of allowance for the instrumental background of the detector is related to the fact that the CXB is virtually isotropic (its fluctuations are no more than 7% on a scale of one square degree and no more than 2-3% on a scale of 20-40 deg. (see, e.g., Schwartz 1970; Schwartz et al. 1976; Warwick et al. 1980; Revnivtsev et al. 2008). Therefore, it is very difficult to separate from the contribution of the instrumental background of the detectors (for more details, see Section 5).

3. The problem of an accurate absolute calibration of the measured flux is related to the limited knowledge of the photon detection efficiency by the detector being used and knowledge of its effective collecting field of view. This problem is considered in more detail in Section 6.

4. THE PROBLEM OF ENERGY CALIBRATIONS

Inaccurate knowledge of the instruments energy calibration inevitably leads to deviations of the measured CXB surface brightness from its true value. For example, a 10% error in the boundaries of the energy channels for the CXB in the energy range 50-300 keV, where its spectral shape can be described by a power law with a slope $\Gamma \sim 2.5$, will lead to an error in the surface brightness of 25-27%!

In the first experiments in the 1960-1970s, there were only a few detector energy channels; there was often no in-flight calibration, which is especially true for the early experiments on the Soviet Kosmos satellites. Under such conditions, 10% or larger uncertainties in the energy calibration were a common occurrence. For example, the attempts to recalibrate the measurements of solar flares made by the scintillation crystals on Prognoz satellites (5, 6, 7, 8) using the measurements of the same events by the instruments with an onboard energy calibration showed that the declared energy scale of the detectors on the Prognoz satellites could be shifted relative to the true one by a factor up to 1.5-2! (Farnik et al., 1984)

The possible variations of the instruments energy scale under the action of various external factors are an additional limitation of the accuracy of its energy calibration. For example, one might expect a change in the energy scale of a gas counter as the gas pressure in it, its temperature, or high voltage changes.

In the detectors based on crystal scintillators with photomultiplier tubes, 10% variations of the energy scale due to the influence of the Earths magnetic field were detected (the HEAO1/A4 experiment; Jung 1989); on CsI(Tl) crystals with photodiodes and based on CdTe semiconductor crystals, a temperature dependence was detected (CsI(Tl), the PICsIT/IBIS experiment of the INTEGRAL observatory (Malaguti et al., 2003); CdTe, the ISGRI/IBIS detector of the INTEGRAL observatory (Terrier et al., 2003). The position-sensitive detectors based on CCD arrays have significant gradients in detector characteristics that should be measured during preflight calibrations and carefully traced during the in-orbit operation of the instrument (see, e.g., Dennerl et al. 2002; Plucinsky et al. 2003; Grant et al. 2012).

Thus, in order that the energy calibration of the detector scale be maximally accurate, it is necessary to provide maximally stable operational conditions for the detectors and to systematically carry out its onboard calibrations.

5. THE INSTRUMENTAL BACKGROUND OF DETECTORS

Measuring the isotropic emission of the sky is a serious problem related to the separation of the flux of X-ray photons arriving from the sky directly at the detector from the count rate of all other particles.

The instrument recording X-ray photons actually counts the following:

- The nearly isotropic (independent of the direction of the instruments field of view) X-ray background flux.

- The events caused by the passage of charged particles (both Galactic cosmic rays and those trapped by the Earths magnetic field) through the detector.

- The fluorescent X-ray photons produced in the detectors construction elements.

- The X-rays and gamma-ray emission from the Earths atmosphere. It can be both the reflected emission from the Sun/CXB/bright X-ray sources and the emission produced by the interaction of cosmic-ray particles with the atmosphere (the so-called Earths albedo emission; Vette 1962). The Compton scattering of gamma-ray photons in the detector body can leave a slight energy in it, which will be perceived as the recording of a low-energy X- ray photon.

- The X-ray and gamma-ray photons emerging during the radioactive decay of construction elements.

- The X-rays (including those from the Sun) scattered in construction elements.

Consider in more details the methods of separation and decrease all these background count rate components of the instrument.

The Background Count Rate Components of Instruments

The instruments recording X-ray and hard X-ray photons count the energy release events in the detector volume. The energy release can result from the passage of both X-ray photons through the detector body and various charged particles. For example, on the Earths surface in the complete absence of X-ray photons, the Geiger counters systematically count about 0.5 count per second per cm^2 . The passage of charged muons produced by the interaction of cosmic-ray protons (with energies above 1-10 GeV) with the Earths atmosphere constitutes the overwhelming majority of the recorded events in this case.

In the upper atmospheric layers, the muon flux decreases, but the flux of Galactic cosmic-ray protons and gamma-ray photons increases. The gamma- ray photons result from the bremsstrahlung of relativistic cosmic-ray electrons and relativistic electrons appearing during the decay of charged muons in the atmosphere (Vette, 1962; Puskin, 1970; Petry, 2005; Sazonov et al., 2008).

Outside the atmosphere, the fluxes of charged particles are represented predominantly by high-energy protons, electrons, and positrons.

The Anticoincidence Shield

A passive shield of detectors with a surface density up to 1 g cm^{-2} efficiently stops the protons with energies below 10 MeV. The penetrating power of higher-energy protons is large enough to pass right through the entire construction of the instrument. This property allowed an efficient method of their filtering to be proposed. The detectors main body is surrounded by additional (anticoincidence) detectors that record the passage of high-energy particles.

The first versions of the anticoincidence shield were based on plastic scintillators. X-ray photons in the energy range 1-10 keV were completely absorbed in the detectors main body (for example, in the gas counter), while high-energy charged particles also passed through the scintillator. The simultaneous triggering of the main detector and the active-shield scintillator served as evidence that the occurred event was related to the passage of a charged particle rather than an X-ray photon.

Using multilayered gas counters was another way of realizing an active anticoincidence shield. Several layers of charge-detecting anodes were passed through the gas-counter volume. The layers of an- odes located at the edges of the detector volume gave a trigger simultaneously with the working layers of the detector if an energetic charged particle passage through the detector.

The efficiency of this method for the filtering of background events in the energy range 1-30 keV depends significantly on the type of the detector used. In the case of a gas counter, the density of the detectors main body is fairly low; therefore, the cosmic-ray protons with an energy of 10 GeV passing through the detector leave an energy falling into its operating range. For example, the gas density for a xenon gas counter operating at a pressure of 1 atm is 5.85×10^{-3} g cm^{-3}, and the mass of the material traversed by the protons at a thickness of the active gas layer 1-2 cm (as, for example, in HEAO1/A2, EXOSAT/ME, GINGA/LAD, RXTE/PCA) is ~ 7 mg cm^{-2}. In this case, the energy lost by the 10-GeV cosmic-ray protons turns out to be $\sim 5 - 15$ keV, falling within the operating range of the instruments. Using an anticoincidence shield in the case of gas counters allows the contribution of the events unrelated to X-ray photons to be reduced by a factor of 100.

The efficiency of the anticoincidence shield for solid-state X-ray detectors (operating at energies be- low 50-100 keV) decreases dramatically, because the mean energy left by the high-energy protons in solid- state detectors with densities of 2-8 g cm^{-3} and thicknesses of 1-2 mm (needed for the absorption of photons with energies up to 70-100 keV) turns out to be several hundred keV. Such events can be filtered out just by the recorded energy release.

The high efficiency of the anticoincidence shield for gas detectors led to the hasty conclusions that all of the remaining events after its use were associated with the real CXB. To illustrate that this is not the case, Fig. 3 presents the spectrum of events recorded in the PCA proportional counter of the RXTE observatory with an anticoincidence shield from all directions. The

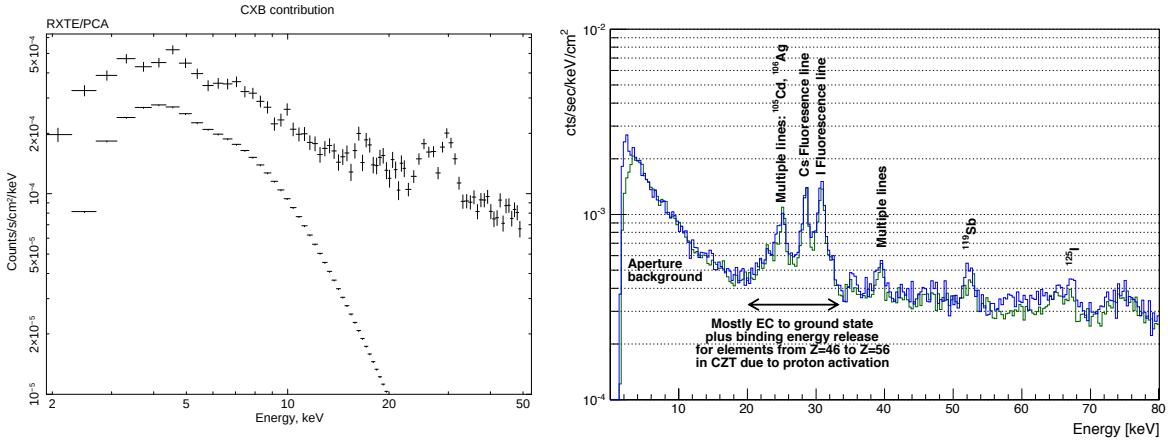

Fig. 3. Distribution of the event count rate in X-ray detectors in the energy left in the detectors main body. In both cases, the detectors were surrounded by an anticoincidence shield. (a) The spectrum of events in the PCA proportional counter of the RXTE observatory. The histogram indicates the CXB contribution. (b) The spectrum of events when observing empty sky fields by the CdZTe semiconductor detector of the NuSTAR observatory (from Harrison et al. 2013. The CXB contribution dominates in the count rate at energies below 20 keV.

count rate of events unrelated to the CXB is seen to be no more than 40-50% of the total one even at energies below 10 keV. Such a CXB measurement error is inadmissible for further studies of the cosmological evolution of black holes in the Universe.

Thus, even when the anticoincidence shields are used, the question about the separation of the contribution of events related to charged particles from the count rate recorded by the detector remains a key one for a reliable and accurate CXB measurement.

Filtering by the Signal Rise Time

Because of the great penetrating power of high- energy charged particles, a charged particle in a geo- metrically large detector ionizes a long trail that pro- duces a long-duration signal in the detecting anodes, considerably longer than that from X-ray photons. This makes it possible to use information about the rise time of the detector signal to separate the events related to the passage of charged particles. This method was proposed in the late 1960s (Gorenstein & Mickiewicz, 1968) and showed a fairly high efficiency Gorenstein et al. (1969).

For solid-state detectors with a large surface density ($> 0.2 - 0.5$ g cm^{-2}), the efficiency of this method is low for X-ray photons at energies below 100 keV. However, this method continues to be used when working with hard X-ray and gamma-ray photons at energies above 200-400 keV (see, e.g., Skelton et al. 2000).

The Influence of Geomagnetic Cutoff Rigidity

Not all of the events related to the passage of charged particles can be filtered out by the anticoincidence shield even if it completely (in the solid angle 4π) covers the recording instrument and through filtering by the detector signal rise time.

The dependence of the measured count rate on various orbital parameters, altitude, position above the Earth, etc. is additionally studied to separate the count rate components related to charged particles. A major factor of the modulation of the count rate of charged particles in this case is their reflection by the Earths magnetic field.

Such a quantity as the magnetic rigidity R can be associated with any charged particle. Particles with the same rigidity move along identical trajectories in the Earths magnetic field:

$$R = \frac{pc}{Ze}$$

here p is the momentum of the charged particle, Ze is its charge, c is the speed of light.

For a particle to be able to descent to a certain altitude above the Earth, its magnetic rigidity must exceed some threshold value. This value can be calculated in the approximation of the Earths dipole magnetic field:

$$R_{\rm cut} = \frac{M \cos^4 \lambda}{r^2[\sqrt{1 + \cos a \cos^3 \lambda} + 1]^2}$$

here λ is the geomagnetic latitude, a is the entrance angle of a positive particle ($\pi/2$ is the vertical motion), r is the distance from the Earths center, and M s the Earths magnetic dipole moment.

The geomagnetic cutoff rigidity can also be written in the form of Stoermers simpler formula:

$$R_{\rm cut} \sim 14.5 \times \left(1 + \frac{h}{r_{\rm E}}\right)^{-2} \cos^4 \lambda \ \ {\rm GeV}$$

Here h is the altitude above the Earths surface, and $r_{\rm E}$ is the mean radius of the Earth. The regions near the equator have the largest geomagnetic cutoff rigidity, $R_{\rm cut} \sim 20$ GeV.

If a particle has a rigidity smaller than that given by the Earths magnetic field in this region, then it cannot reach the Earths surface and will be reflected back into the space. Thus, it turns out that the charged cosmic-ray particles with energies 1–20 GeV constituting the bulk of the cosmic rays in interplanetary space reach the Earths surface differently; the fluxes of these charged particles are different in different places of the Earth. Both the rate of cosmic-ray passage through the detectors body and its illumination by the hard X- ray and gamma-ray emission from the Earths atmosphere (arising from the interaction of cosmic rays with the atmosphere) will depend on the magnetic rigidity in which the instrument is at a given instant.

By investigating the dependence of the instruments count rate on magnetic rigidity, one can at- tempt to separate the CXB contribution from the charged-particle contribution. The experiments on the Soviet Kosmos-135 (1966–1967), 163 (1967), and 461 (1971–1979) satellites (Golenetskii et al., 1971; Mazets et al., 1975) can be considered as an example of this approach. In these experiments, an omnidirectional detector located at a certain distance from the satellites main body (to reduce the contribution from the induced radioactivity of the satellite material) carried out measurements in different parts of the orbit, at different magnetic rigidities. The detector count rate was assumed to be the sum of the CXB contribution independent of the magnetic rigidity and the contribution of the Earths induced emission dependent on the magnetic rigidity of the region above which the satellite flies at a given instant.

Subtracting the contribution of the count rate dependent on geomagnetic cutoff rigidity allowed the CXB to be estimated. In order to additionally get rid of the contribution of the emission from the detectors induced radioactivity, the authors used the observations performed immediately after the satellite launch until its first passage through the South Atlantic Anomaly.

In fact, the described method allows only an upper limit for the CXB surface brightness to be determined, because the possibility that some part of the detectors instrumental background is not modulated by the geomagnetic cutoff rigidity remains anyway. This may have become the reason why the CXB measurements from the Kosmos-135, 163, and 461 satellites gave slightly larger surface brightnesses than other experiments.

The Absorption of X-ray Photons in the Upper Atmospheric Layers

In some rocket experiments, attempts were made to separate the contribution of the events related to the passage of charged particles from the events related to X-ray photons by measuring their different dependence on the depth of the residual atmosphere.

For example, in the experiments carried out in September 1966 by a group from the Lawrence Radiation Laboratory of the US Department of Defence and the University of California (Seward et al., 1967), it was pointed out that the count rate of the detectors anticoincidence shield was approximately the same at altitudes of about 120 and 40 km. This was used as a basis for the assumption that the effects related to the passage of charged particles through the instrument are identical at these altitudes (in fact, this is true only partly, because the compositions of charged particles at these altitudes are fundamentally different; therefore, their influence on the instrument can be different). However, the flux of X-ray photons must be absorbed by the residual atmosphere above the rocket at an altitude of 40 km. Subtracting the instruments count rates at these two altitudes gave the authors an estimate of the CXB surface brightness.

Radioactivity

Energetic cosmic-ray particles are responsible not only for the events recorded during their direct passage through the instrument. A very important component of the background event count rate for virtually any instruments is the count rate of particles resulting from the decay of radioactive elements produced in the construction of the instrument or satellite when they are irradiated by protons from the Earths radiation belts. The concentration of such protons is highest in the subpolar regions and in the region of the so-called South Atlantic Anomaly, the region in which the lower van Allen radiation belt is closest to the Earth.

The specific set of elements passing into a radioactive state depends on the design of the spacecraft and the detector. After the passage through a region with a high flux of energetic protons, the detector count rate rises abruptly, although it must decline exponentially with a characteristic time corresponding to the decay time of the radioactive element (see, e.g., Fig. 4). In some cases, the range of characteristic times of the exponential decline in the instruments

background count rate can be identified (as, for example, for the LAC/GINGA (Hayashida et al., 1989) and PCA/RXTE (Jahoda et al., 2006) proportional counters and NaI(Tl)-based scintillators (Jung, 1989).

In other cases, it turns out that the number of decaying radioactive elements is large enough and the total background count rate declines already not exponentially but according to a power law (Dennis et al., 1973). In some experiments (for example, OSO-3 and OSO-5), it was found that long-term trends of an increase in the detector count rate occasionally exist, suggesting the accumulation of a large number of long-lived radioactive isotopes.

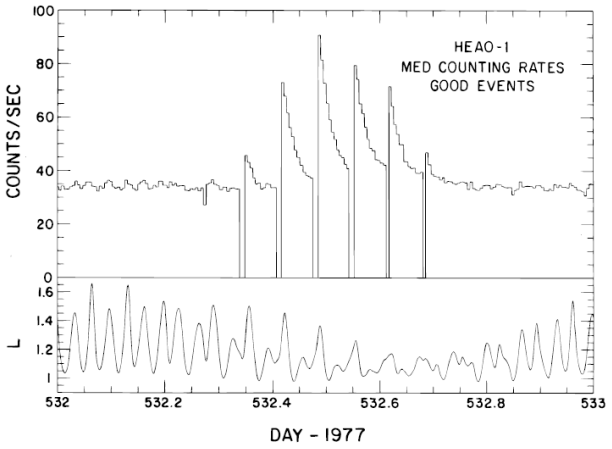

Fig. 4. Example of the count rate from the A4/MED detector (80-2000 keV) onboard the HEAO1 observatory on one of the days. The background count rate is seen to increase sharply after the passage through the South Atlantic Anomaly. The radioactive elements produced in this period (mainly ^{128}I from the NaI scintillator crystal nuclei with a half-life of about 25 min) then decay, leading to an approximately exponential decline in the count rate. From Kinzer et al. (1997).

The measurements made, for example, on OSO (Orbital Solar Observatory) satellites showed that ignoring the contribution of the events due to radioactive elements (activation) led to a considerable overestimation of the derived CXB surface brightness. An example of such measurements is shown in Fig. 6.

Blocking the Instruments Aperture

The most obvious way to measure the contribution of the events unrelated to the passage of X-ray photons from the sky through the instrument is a modulation of the instruments aperture, i.e., a periodic blocking of the aperture by a passive or active shield layer. If the aperture opening and closing cycle is short enough, then it can be assumed that the back- ground event count rate in these periods is the same, but the instrument sees an additional contribution of the flux

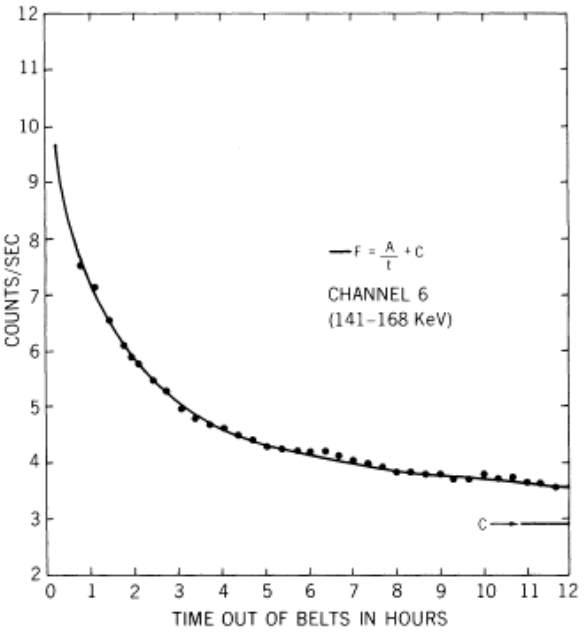

Fig. 5. Mean count rate of the detector in the energy range 141-168 keV as a function of the time since the last passage through the South Atlantic Anomaly. The solid curve indicates a gradual decline in the count rate with time (from Dennis et al. 1973).

of X-ray photons from the sky in the case of an open aperture. A cover made of a material opaque to X-ray photons in the energy range being investigated can play the role of a passive shield.

One of the first such measurements was made in late 1965 in a balloon-borne experiment. A NaI(Tl)- based scintillator surrounded by an anticoincidence shield scanned a 20 deg sky region, and its field of view was periodically, with a period of 100 s, blocked by a rotating 2-mm-thick tin cover. The CXB flux in the energy range 26-90 keV was measured as a result of these experiments (see Fig. 7).

Similar experiments on rockets were carried out by a group from the Nagoya University (Fukada et al., 1975). In late 1970-early 1971, a methodologically similar experiment was carried out onboard Lunokhod 1 during its operation on the lunar surface. The scientific equipment of Lunokhod 1 included the RT-1 collimating X-ray telescope consisting of two gas counters with an effective area of 6.5 cm 2 (with a two-layer system of anodes for the anticoincidence shield) and a collimator limiting a 3.3-deg field of view. The effective operating range of the detectors is 1-6 keV. To separate the contribution of charged particles from the total count rate of the detectors, the aperture of the two counters should have alternately been covered with a 10- iron filter blocking the X-ray photons. Un-

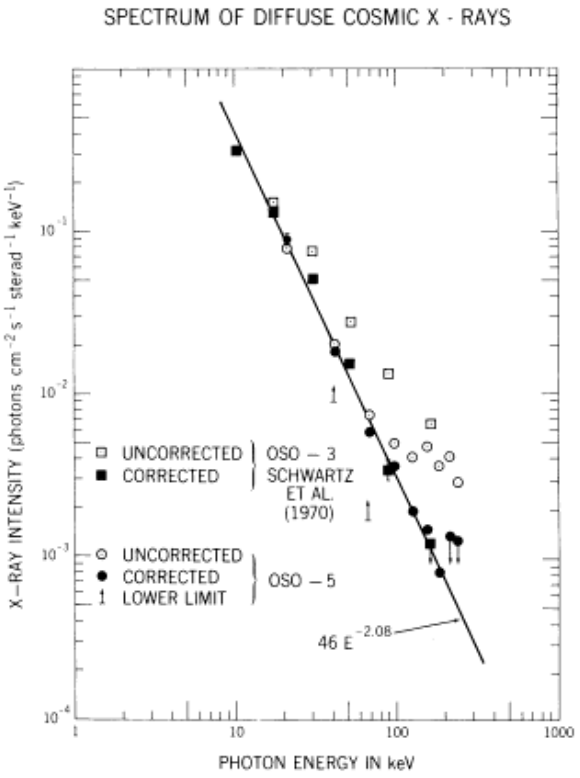

Fig. 6. CXB spectra from the results of OSO-3 and OSO-5 satellite measurements. The spectra of the events selected after various filterings of the measurements are indicated by the open symbols. The filled symbols indicate the results of the CXB measurements obtained after additional corrections for the possible contribution from the decay of radioactive elements (from Dennis et al. 1973).

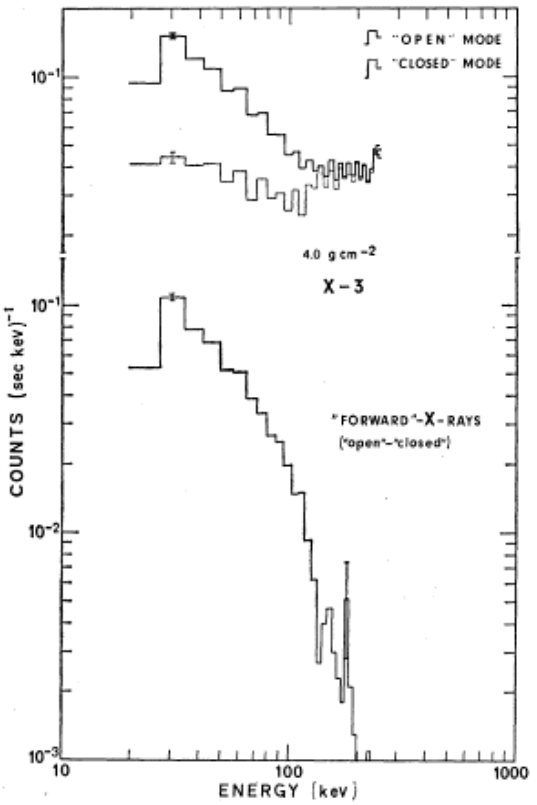

Fig. 7. Spectra of events measured with a scintillator when measuring the CXB in the regimes of an open and closed aperture and their difference (from Bleeker & Deerenberg 1970)

fortunately, during the operation of the instrument on the Moon, it turned out that the filter was not transferred from one counter to the other, which did not allow scientific results from this experiment to be obtained.

Using identical detectors when observing the same sky field but with one of them being blocked (for example, by an additional absorbing layer) to prevent the recording of X-ray photons can serve as another realization of this approach. In this way, the CXB surface brightness was measured on the Luna-12 interplanetary spacecraft in 1966 (Mandel'Shtam & Tindo, 1967). In this experiment, the apertures of two virtually identical Geiger counters were covered with aluminium (10 μm) windows, but one counter was additionally covered with a silver-gold foil filter making it insensitive to X-ray photons. Comparison of the count rates from the two counters made it possible to estimate the CXB surface brightness in the energy range 1-6 keV.

A significant shortcoming of this approach is the limited identity of any devices. As a result, the actual background count rates in two different detectors may be considered identical only with a certain accuracy. If this accuracy exceeds the amplitude of the useful signal expected in the detector with an open aperture, then this method of estimating the detector back- ground turns out to be unreliable. For example, in the Pulsar X-1 hard X-ray experiment on the Kvant module of the Mir Space Station, an attempt was made to use one of the NaI(Tl) scintillators to estimate the background count rate of other scintillators. The accuracy of this method turned out to be unsatisfactory and, therefore, attempts were made to determine the background count rate of the detectors in real observations by shifting the field of view of the detector with an open aperture, i.e., by alternating the observations of the source and background fields (see, e.g., Syunyaev et al. 1994).

Blocking the Aperture by an Active Shield

In the method with aperture blocking, there is a possibility that a change in the configuration will lead to a change in the count rate of the detector background

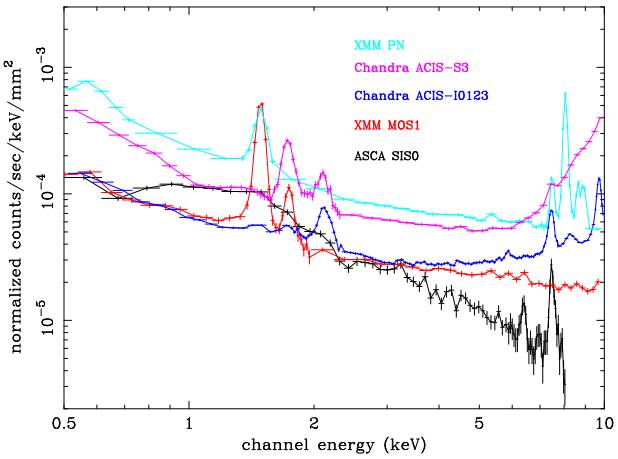

Fig. 8. Instrumental background spectrum for the ASCA, Chandra, and XMM-Newton detectors. The contribution from the fluorescent lines of the detector materials is clearly seen at energies ∼1.5 (Al-K), 1.74 (Si-K), 2.123 (Au-M), 5.89, 6.49 (Mn-K), 7.48 (Ni-K), 8.05,8.91 (Cu-K), 8.64, 9.57 keV (Zn-K). The instruments are listed in the figure in order of decreasing background intensity level at an energy of 5 keV (from Katayama et al. 2004).

illumination. Theoretically, this is possible, because: first, high-energy cosmic rays create induced radioactivity in the material of the detector or satellite and in the material of the cover or collimators; second, the cover or collimators can themselves be the sources of X-ray emission, for example, through fluorescence.

An example of the presence of fluorescent lines from the material of the detector or its environment can be seen in Fig. 8, which shows the actual instrumental background spectrum for the ASCA, Chandra, and XMM-Newton detectors (from Katayama et al. (2004)).

The fact that the appearance of an additional cover in the detector aperture could affect the measurements at energies above several hundred keV was demonstrated in laboratory experiments (for a description, see Kinzer et al. 1997). To reduce the influence of this effect, not only a passive shield blocking the aperture but also an active shield was used in some experiments. An element similar to the antico- incidence shield, for example, CsI-based scintillators, was used to cover the aperture. The events related to the passage of charged particles through such a cover are additionally cut off by the anticoincidence scheme.

One of the first such experiments was carried out during the flight of a stratospheric balloon on October 17, 1973, by a group from the US Naval Research Laboratory (Kinzer et al., 1978). Studies showed that the effect from the activity (the anticoincidence operation) of the cover blocking the detector aperture at energies below 100-150 keV is small, less than 15%, i.e., using an active or passive shield to block the instruments aperture changed the derived CXB sur- face brightness by no more than 15%. More detailed studies using the analogous 4/MED experiment but installed on the HEAO1 satellite and, therefore, making measurements for many months showed an even smaller effect from the activity of the blocking cover up to energies of several hundred keV (Kinzer et al., 1997).

Modulation of the Instruments Field of View

The instruments aperture can be changed not only in variant 0 or 1 (open or closed) but also in more steps. A two-step change in the instruments field of view was made in balloon-borne experiments by a group from the Nagoya University (Makino, 1975). A four-step ($60° \times 38.6°$, $21° \times 38.6°$,$6.2° \times 38.6°$, and completely closed) change of the instruments field of view was made in a rocket experiment in 1967 by a group from the Tokyo and Nagoya Universities (Matsuoka et al., 1969). Measuring the component whose flux depends linearly on the size of the field of view open to the detector gave an estimate of the CXB spectrum in the energy range 3.6-9 keV. The field of view of the recording instrument was modulated in more steps in a series of rocket experiments in the energy range 2-20 keV by a group from the NASA Goddard Space Flight Center in 1968–1969 (Boldt et al., 1969, 1970). In these experiments, the gas counter was placed behind the collimating system in which some (in the same direction) of the collimating plates provided a 14° field of view, while the collimating plates in the perpendicular direction could occupy 10 different positions, providing a set of different effective solid angles, up to 0.17 steradians, scanned by the detector in the sky. The flux directly proportional to the solid angle in which the measure- ments occurred gave an estimate of the isotropic CXB surface brightness.

The technology of using a variable field of view of the instrument to measure the CXB achieved its greatest progress with the CXE/A2 experiment of the Goddard Space Flight Center (Rothschild et al., 1979) onboard the HEAO1 observatory (1977-1979). The instrument consisted of six gas counters that jointly covered the energy range 0.15-60 keV. The entrance aperture of the detectors was specified by a system of collimators with an alternating size of their field of view. The first and second halves of the charge- detecting anodes were illuminated through the collimators limiting a field of view with a certain size and a field of view approximately twice as large in size, respectively. Two HED detectors (2.6–60 keV) had $\sim 3 \times 3$ and $\sim 3 \times 6$ deg fields of view; two LED detectors (0.15-3 keV), one MED detector (1.5-20 keV), and one HED

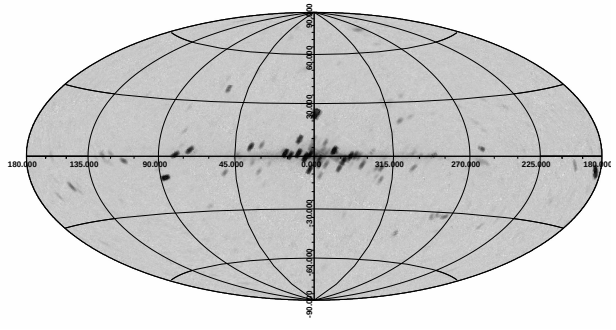

Fig. 9. Sky map from the measurements with the CXE/A2 instrument onboard the HEAO1 orbital observatory. The map is shown in the Aitoff projection in Galactic coordinates. The straight line passing horizontally through the center of the map is the Galactic equator. Since the angular resolution of the instrument is finite, the bright sources on the map are seen as $3^\circ \times 6^\circ$ spots. The gray color in the bulk of the sky is the CXB accumulated by the CXE/A2 instrument in its $3^\circ \times 6^\circ$ aperture.

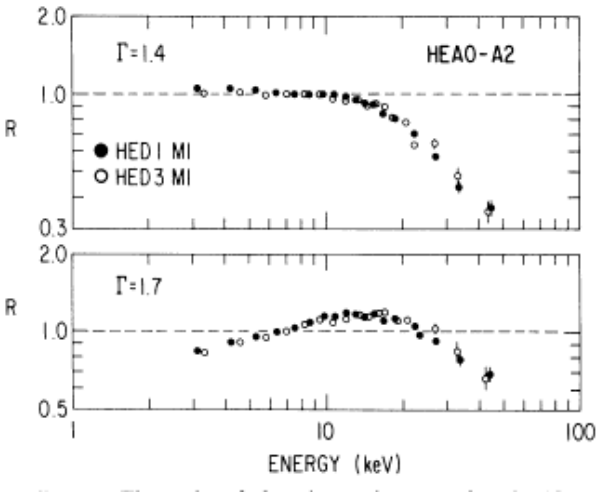

Fig. 10. Shape of the CXB spectrum from the measurements in the 2 experiment onboard the HEAO1 observatory. The ratio of the spectral CXB surface brightness density to the model of its power-law energy dependence $dN/dE \propto E^{-\Gamma}$ is shown (from Marshall et al. 1980).

detector had $\sim 3 \times 3$ and $\sim 3 \times 1.5$ deg fields of view. Alternating the fields of view above different anodes provided an almost identical background count rate in these anodes at a CXB flux differing by a factor of 2. Subtracting the measure- ments of one set of anodes from the measurements of the other set of anodes allowed one to make an ideal subtraction of the instrumental background and a reliable CXB measurement (Marshall et al., 1980). These measurements are still deemed to be among the most reliable ones in the energy range 2-60 keV. The difficulty of determining the absolute calibration of the measured flux remained a significant problem in this case. Some time ago, an attempt was made to re- calibrate these CXB measurements using the observations of the Crab Nebula (Revnivtsev et al., 2005).

Low-Energy Electrons and Protons

The low-energy (below 1 MeV) electrons that, when passing through the detector designed to record X-ray photons, leave an energy falling into the instruments operating range are one of the important components of the charged particle flux in space. Thus, these electrons also produce the background count rate in the instrument.

The problem of keV electrons was found back in the early 1970s in rocket experiments (see, e.g., Seward et al. 1974).

The instruments designed to investigate the low-energy (below several keV) X-ray emission and, therefore, having very thin aperture windows (for ex- ample, formvar films with a thickness of 0.06 mg cm^{-2}) were found to often record the fluxes of low-energy electrons. The fluxes of such electrons influence significantly the quality of cosmic X-ray emission measurements (an example of this influence in the rocket experiment on May 2, 1972, by a group from the Livermore National Laboratory of the US Department of Energy is shown in Fig. 11). Therefore, attempts were made to reduce their fluxes by various methods, for example, by applying electrostatic and magnetic fields to deflect the electron trajectories from the detector.

The numerous rocket experiments carried out under various conditions showed the following (Seward et al., 1974):

- The electrostatic cutoff of electrons by applying a voltage to the collimators does not give the necessary effect. A high voltage applied to the collimators leads to the generation of soft X- ray photons, which creates more background events than it allows them to be cut off.
- The magnetic cutoff of electrons works very well. At magnetic fields up to 100 G, from 90 to 99% of the electrons up to energies of several tens of keV are cut off.
- Highly polished collimators were found to additionally focus low-energy electrons into the detector body. The rough collimator surface in this case is a good way to combat this effect.

With the advent of telescopes with grazing- incidence mirrors capable of focusing X-ray photons with energies up to 10 keV, the problem of low-energy charged particles became even more topical. Apart from photons, such mirrors also efficiently focus low-

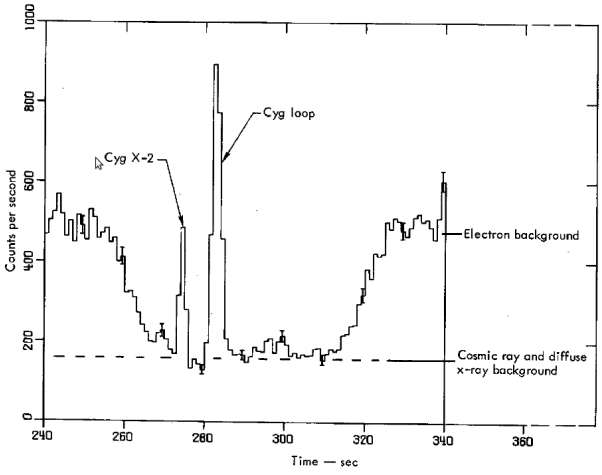

Fig. 11. Detector count rate in the rocket experiment on May 20, 1972, when scanning through the Cygnus region. The background count rate produced by electrons is seen to be twice the background count rate from the X-ray background and charged cosmic-ray. The detector aperture was covered with a formvar layer 0.035 mg cm^{-2} in thickness. The detector count rate in the energy range 0.2-4 keV is shown (from Seward et al. 1974).

energy (up to several tens and hundreds of keV) electrons and protons, increasing significantly the flux of charged particles on the detector.

For example, such an increase in the flux of protons with energies of ∼100–200 keV led not only to a rise in the detector background count rate but also to a significant degradation of the receiving X- ray CCD array mounted at the focus of the Chandra telescope (Prigozhin et al., 2000).

Various configurations of magnetic deflectors are currently used to reduce the flux of charged particles with energies up to 100 keV. In particular, such deflectors were mounted on the optical system of the ROSAT observatory; at present, they are mounted on the optical systems of the Chandra, XMM, and SWIFT/XRT observatories (for a description, see, e.g., Spiga et al. 2008). The magnetic fields achievable at present on the small magnets of such deflectors (up to 1 kG) do not allow the problem of irradiation by protons with energies above 50-100 keV to be solved.

Another way to solve the problem with the irradiation of a recording detector by low-energy charged particles is to cover the entrance window of the detector with a protective layer of material capable of stopping the charged particles. In latest generation gas spectrometers, an additional propane layer provides protection against low-energy electrons (see the RXTE/PCA detector scheme; Jahoda et al. 2006). The semiconductor detector based on CdZnTe crystals onboard the NuSTAR observatory is covered with a 110-μm-thick beryllium window, which allows the electrons up to energies ∼100 keV and the protons up to energies of less than 1 MeV to be absorbed. On the ART-P X-ray telescope of the GRANAT orbital observatory (1989-1998), a 500-μm-thick beryllium window performed the same role.

An interesting method for separating the contribution of low-energy electrons and photons with energies 1-7 keV was applied in one of the detectors onboard the OSO-8 solar observatory (1975-1978). The entrance window of the gas counter of detector B in the CXS (Cosmic X-ray Spectroscopy experiment) experiment of the NASA Goddard Space Flight Center was covered with protective layers of different thicknesses. The entire detector was covered with a 50-μm-thick beryllium layer. In addition, one half of the detector was covered with a 30-μm-thick beryllium layer, while the other half was covered with a 20-μm-thick aluminium layer. These additional thicknesses of the protective layers were chosen so that the thickness of the entire protective layer in units of g cm^{-2} was the same. Thus, the protective layers of the two halves of detector B in the CXS instrument transmitted the low-energy electrons virtually identically and the photons with energies up to ∼7 keV differently (Pravdo, 1976). The CXB was measured using this difference.

Blocking the Aperture by the Earth

Using the Earth as a screen to cover the instruments aperture is an important way to separate the count rate of events unrelated to the cosmic X-ray emission and the CXB emission. The Earth unlit by the Sun is a source of X-ray emission due to the CXB reflection from its surface and due to the emission arising from the interaction of high-energy cosmic rays with the Earths atmosphere (Schwartz & Peterson, 1974; Sazonov et al., 2007; Churazov et al., 2007, 2008; Ajello et al., 2008).

The sunlit atmosphere of the Earth additionally radiates due to the reflection of the solar flux (see Fig. 12). It can be seen from Fig. 12 that the Earths night side is a very faint source of X-ray emission up to energies of several tens of keV. Thus, the Earths night side can (1) serve as a very efficient screen for the CXB, (2) give little intrinsic X-ray emission (the surface brightness of the night-side Earth can be lower than the CXB one by tens of times), and (3) is also an opaque screen for cosmic rays, which is very difficult to achieve with ordinary screens/covers in instruments.

The observations of the Earths night side have been used very actively to measure the instrumental background of X-ray detectors since the early 1990s (for example, for the ASCA (Gendreau et al., 1995) and BeppoSAX (Parmar et al., 1999) orbital observatories; the Moons night side is used, for example, to

calibrate the background of the Chandra orbital observatory (Markevitch et al., 2003).

In 2003, the observations of the Earths night side were used to measure the CXB with the collimated PCA spectrometer onboard the RXTE observatory (Revnivtsev et al., 2003).

In 2006, a special series of INTEGRAL observations of the Earth was performed to measure the CXB in the energy range 5-200 keV (Churazov et al., 2007). The INTEGRAL observatory flies in a highly elliptical orbit with an apogee of ∼150 000 km. From such a distance, the Earth occupies only less than 5 deg. in the sky, while the fields of view of the main instruments are 15 and 20 deg. Therefore, to maximize the useful signal (the total CXB flux eclipsed by the Earth), the INTEGRAL observations of the Earth were carried out in a period when the distance from the Earth was 40 000–100 000 km (Churazov et al., 2007).

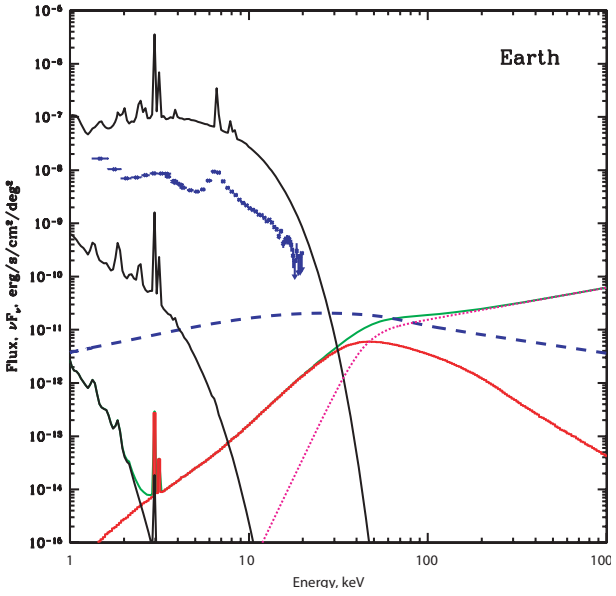

Fig. 12. X-ray spectrum of the Earths surface. The dashed curve indicates the spectrum of the incident CXB emission. The lower solid curve indicates the contribution of the reflected CXB emission, the dotted curve indicates the contribution of the so-called albedo emission arising from the interaction of high-energy cosmic rays with the atmosphere, the solid (black) curves in the left part of the figure indicate the contribution of the solar emission reflected from the atmosphere at three levels of solar activity: in quiescence (lower curve), at maximum solar activity (middle curve), and in a flare (upper curve; the possible contribution from the nonthermal component of the solar emission is disregarded here). The asterisks indicate the spectrum of the Earths day side in the case of an active Sun from the RXTE measurements (from Churazov et al. 2007).

At energies above 10 keV, the CXB measurements using eclipses by the Earth are already complicated significantly by the contribution of the Earths intrinsic hard X-ray emission (see Fig. 12). This contribution was taken into account by modeling the shape of the Earths spectrum Sazonov et al. (2007); Churazov et al. (2007).

A much stronger useful signal from the CXB covering by the Earth can be measured on satellites in low near-Earth orbits (at altitudes of ∼500 km). Such measurements were made with the currently largest hard X-ray BAT telescope onboard the SWIFT observatory with an effective area of more than 2000 sq. cm (Ajello et al., 2008). However, despite the fairly high statistical significance of these measurements, the technique itself used to determine the CXB at energies above 10-20 keV suggests the existence of a certain systematic error – subtracting the contribution of the Earths intrinsic emission is required.

The conclusion follows from all of the aforesaid that the CXB spectrum in the energy range 5–70 keV, which is of great importance for determining the fraction of hidden (absorbed) AGNs in the Universe, particularly at high redshifts, is currently known with an unsatisfactory accuracy and requires a refinement. It is especially important that the measurements at energies below 10-15 keV and above 15-20 keV are systematically carried out by different instruments with different systematic errors and different absolute calibrations. Therefore, properly joining the measurements in these energy ranges is a very important problem when measuring the true CXB brightness (for a discussion, see, e.g., Moretti et al. 2009).

6. THE PROBLEMS OF ABSOLUTE CALIBRATION OF CXB BRIGHTNESS MEASUREMENTS

Once the contribution of the events unrelated to the X-ray photons passing through the instruments entrance aperture has been taken into account, it is necessary to properly recalculate the recorded count rate to the true CXB surface brightness.

There are several series problems in this way:

- The absolute calibration of the detector efficiency.
- Determining the effective solid angle in the sky from which the CXB flux is collected

The Absolute Calibration of the Detector Efficiency

Determining the absolute detector efficiency is a big technical problem for almost any X-ray instruments. As a result, the flux from the same astrophysical source measured at the same time turns out to be different in different experiments. To avoid this problem, it is necessary to carry out a series of calibration measurements in laboratories that would allow the absolute

efficiency of the detectors, their correct effective area, etc. to be estimated.

The effective area of an instrument can often be estimated with accuracies of 10-20% through theoretical calculations of the photon detection process by taking into account all the necessary physics and geometry of the instrument. First of all, it is necessary to take into account maximally accurately the distribution of events in the detector in energy channels dependent on the incident photon energy. Then, it is necessary to determine the quantum efficiency of the detector and its individual elements (if the detector is a position-sensitive one). At present, these calculations are often performed using software packages specially developed to properly take into account the various physical processes during the interaction of photons (and other particles) in the material, for example, the GEANT software package http://geant4.cern.ch/ (for examples of calculations, see Prigozhin et al. 2003; Godet et al. 2009).

Additional precise measurements are needed to achieve an absolute accuracy better than 10%. At energies below 4-7 keV, such precise measurements are often made using a synchrotron source of photons whose absolute brightness can be accurately calculated given the current of electrons in the accelerator beam used (see, e.g., Bautz et al. 2000; Krumrey et al. 2004). However, an absolute calibration accuracy for the instrument better than 5% can rarely be achieved even after these efforts.

At energies above 4-7 keV and for geometrically large detectors, such measurements can no longer be made. Instead, a set of different radioactive materials with known values of their activity are used to mea- sure the absolute efficiency of X-ray detectors (see, e.g., Barthelmy et al. 2005).

Despite the great efforts put by the groups of instrument developers to obtain good absolute calibrations of their instruments, it turns out that the absolute accuracy of the measured fluxes from astrophysical sources is low in real experiments. One way to combat this problem is to use some astrophysical object with known characteristics to determine the properties of an X-ray instrument. For example, attempts are made to determine the parameters of soft X-ray instruments in this way using the spectra of hot white dwarfs and isolated neutron stars (see, e.g., Beuermann et al. 2007).

The cross-calibration of various X-ray instruments is often made by observing one of the brightest sources in the X-ray sky, Tau -1 (the Crab Nebula). This object is an isolated bright young pulsar in an X- ray bright nebula (the Crab Nebula). The spectrum of this source (pulsar+nebula) has no emission features and can be well described by a simple power law with a photon index $\Gamma \approx 2.1$ in a wide energy range (1-100 keV). Numerous observations of this source with various instruments show that its flux is essentially constant and it can be effectively used to test the calibrations of various instruments (Toor & Seward, 1974; Kirsch et al., 2005). It should be noted, however, that small variations of its flux on a scale of 4-6% have recently been detected (Wilson-Hodge et al., 2011), which should be kept in mind when performing cross-calibrations with an accuracy better than 5-7%.

The source Tau X-1 gives a flux of $\sim 10^{-8}$ erg s^{-1} cm-2 and is too bright for almost all latest-generation focusing X-ray telescopes. To make the cross-calibration of these instruments, attempts are made to use other astrophysical sources whose flux should not vary significantly over tens of years, for example, supernova remnants. Such observations show that the problem of the calibration accuracy for instruments still remains fairly serious: for example, Tsujimoto et al. (2011) and Ishida et al. (2011) showed that the discrepancies in fluxes from the same source could reach 20% in the energy range 2-8 keV and 46%(!) in the range 15-50 keV.

Determining the Effective Solid Angle

An additional significant problem of determining the CXB surface brightness is an accurate determination of the effective solid angle from which the CXB photons are collected. Two main effects in this case are vignetting and stray light.

Vignetting is a reduction in the flux from a source recorded by the detector as it recedes from the center of the field of view. In the case of detectors whose field of view is limited by a system of collimators, vignetting simply determines the instruments field of view: the recorded flux from a point source in the sky decreases linearly as it recedes from the center of the field of view; the recorded flux from the source at the edge of the field of view is zero. In the case of focusing telescopes, the field of view is determined by the detector size in the focal plane of the optical system and by the properties of the focusing system. Typically, the magnitude of the vignetting effect for such systems is 70-80% at the edge of the field of view. The vignetting effect is fairly easy to measure by performing a set of observations for a constant source in the X-ray sky at different positions in the instruments field of view.

The stray-light effect is much more difficult to take into account. It arises from the fact that the photons arriving from regions outside the instruments field of view and through the reflections that are not envisaged in its design fall on the X-ray detector.

For example, these can be the photons reflected from the collimator walls (see, e.g., Dumas et al. 1972) or the photons that passed through the slits in the detectors active or passive shield. Figure 13 shows a

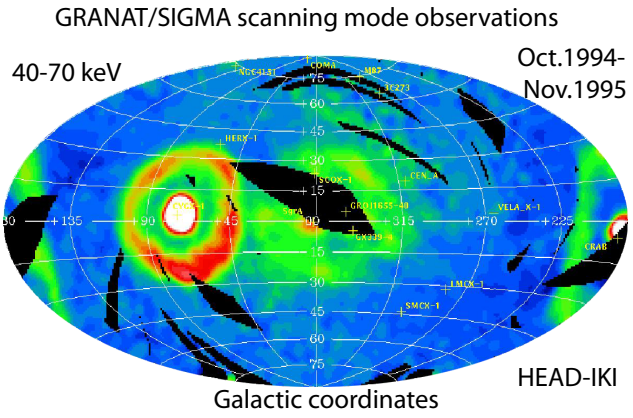

Fig. 13. Illustration of the existence of stray light in the hard X-ray SIGMA telescope. The all-sky map obtained with the SIGMA telescope onboard the GRANAT observatory during scanning observations in 1994-1995 is shown (Churazov and Gilfanov, private communication). Bright sources in the hard X-ray sky, the Crab Nebula and Cygnus X-1, are seen; the total emission from the sources in the Galactic center region is seen. In addition, however, rings are clearly seen around the bright sources arising from slits in the telescopes shield.

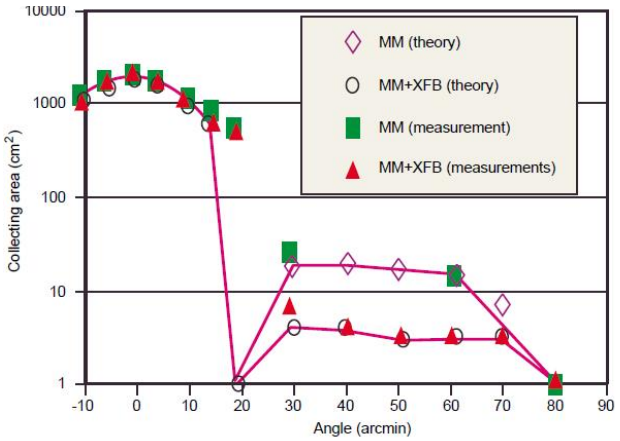

Fig. 14. Collecting area of one mirror system in the -Newton telescope. The mirror system is seen to continue to concentrate the photons on the detector from sources far (up to a distance of 1.5 deg.) beyond the edge of the telescopes field of view (about 15 arcmin). From de Chambure et al. (1999).

good example of the presence of such stray- light photons for the hard X-ray SIGMA telescope onboard the GRANAT observatory. It can be seen that apart from the photons incident on the detector through the instruments main field of view (the spots around the positions of bright sources in Fig. 13), there exists a flux of photons incident on the detector from a direction of ∼25-30 deg. from the center of the main field of view (the circles around the positions of bright sources). This flux is associated with the existing slits in the telescopes lateral shield (Claret et al. 1994).

In focusing telescopes, stray light can arise due to the direct (without any reflection from the mirrors) falling of photons from the X-ray sky, due to the photons that experienced one reflection (see, e.g., de Chambure et al. 1999), or due to the photons that arrived from outside the mirror system (as, for example, in the NuSTAR telescope with an open mirror system; Wik et al. 2014). Such stray light manifests itself in the fact that the focal detector of the X-ray telescope sees the X-ray photons from a source far outside the telescopes field of view. The fraction of X-ray photons from sources outside the field of view depends on its design, on the presence of additional protective baffles. The stray light produced on the detector of the -Newton telescope by a constant source at various distances from the center of the field of view is shown in Fig. 14.

It can be concluded that the stray light on the detector is produced by the convolution of the CXB surface brightness with the response of the telescope+detector system dependent on the vignetting $f_{\rm vign}$, which reduces the effective solid angle from which the CXB flux is collected, and on the stray light $f_{\rm sl}$, which increases the effective solid angle from which the CXB is collected, as follows:

$$F = \int I_{\rm CXB}(f_{\rm vign} + f_{\rm sl})d\Omega$$

Since the CXB surface brightness is virtually in- dependent of the direction in the sky, the convolutions in this expression can be recalculated to a simple product of the integrated vignetting and the integrated stray light with the CXB surface brightness.

Measuring these characteristics for a real instrument is a very important factor determining the CXB measurement accuracy (see, e.g., Moretti et al. 2009). Scanning observations of the sky often allow the vignetting and stray-light effects to be measured directly from observational data by analyzing the fluxes of constant sources in the sky, for example, the Crab Nebula (Revnivtsev et al., 2005; Jahoda et al., 2006). Special series of observations are performed for a reliable measurement of these effects in mirror telescopes, and the authors try to take them into ac- count as accurately as possible (see, e.g., Moretti et al. 2009).

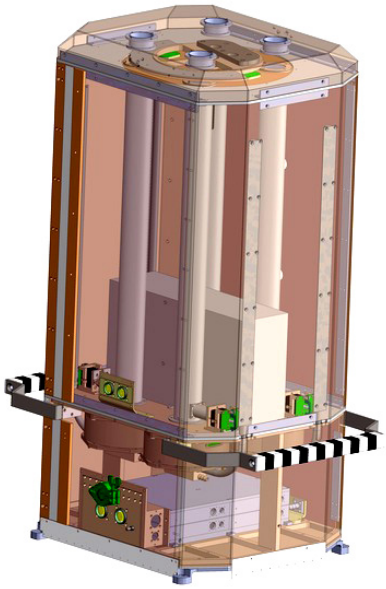

Fig. 15. General view of the MVN experiment. The main objective of the experiment is to measure the CXB surface brightness with the maximum possible accuracy in the energy range 6-70 keV. The reliability of allowance for the instrumental background of the detectors will be provided by periodically blocking the detector aperture by a rotating wheel (in the upper part of the instrument); the stability of the energy scale and efficiency of the detectors will be controlled by the observations of the calibration sources being periodically inserted into the field of view of the detectors (the inserts in the lower part of the collimators). Thermal stabilization is created by the thermal control unit (the system control is located in the box between the collimators).

7. THE MVN (MONITOR VSEGO NEBA) EXPERIMENT

The MVN (Monitor Vsego Neba, translates as the all-sky monitor) experiment has been proposed by the Space Research Institute of the Russian Academy of Sciences and is being developed in collaboration with the Energia Rocket and Space Corporation to measure the CXB surface brightness in a wide energy range, 5-70 keV (Revnivtsev et al., 2012).

The MVN instrument (see Fig. 15) is planned to be mounted on the external platform of the Russian segment of the International Space Station (ISS). Its orientation will be fixed, and the instruments field of view will be directed to zenith. As a result of the evolution of the ISS position with time, the instruments field of view will gradually cover different areas in the sky and and will cover the entire reachable part of the celestial sphere, ∼83% of the entire sky or 32.4×10^3 sq. deg., over a period of about 72 days. The reachable part of the sky will be covered ∼15 times over three years of the instruments planned operation.

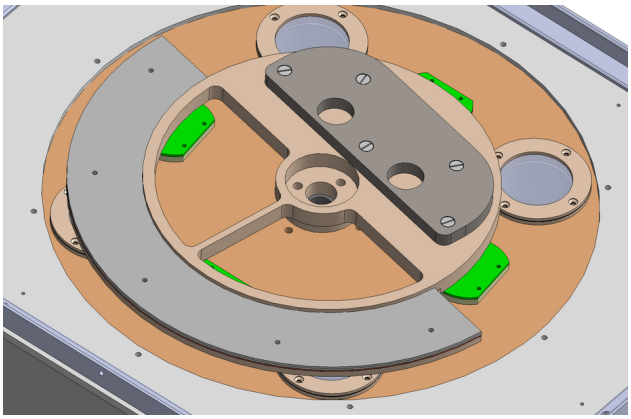

Fig. 16. View of the entrance windows of the collimators in the MVN experiment and the rotating modulating wheel.

The main parameters of the MVN experiment are:

Table 1. Main parameters of MVN experiment

Crystal	CdTe
Crystal thickness	1 mm
Energy band	5-70 keV
Field of view	∼3.2° diameter
Effective area	4×4.5 cm^2
Operational temperature	−30°C
Time resolution	1
Power consumption	40 W

The MVN instrument consists of four identical semiconductor CdTe detectors placed under cylindrical collimators limiting a field of view 3.2 deg. in diameter. The collimators are made of three metal layers, each with a thickness of 1 mm; from the outside inward, the layers are tin, copper, and aluminium. The sequence of metals in the collimators was chosen so that the fluorescent lines arising in the outer parts of the collimator were absorbed in the inner ones, while the fluorescent lines of the inner layer (aluminium at an energy of ∼1.56 keV) were outside the operating range of the instrument. The detector crystals are surrounded by the same multilayered passive shield with a surface density of ∼1.9 g cm^{-2}. The shield transparency is no more than 3% for photons with energies below 70 keV.

Since the goal of MVN is to measure the cosmic X-ray background maximally reliably and accurately, all the difficulties of CXB measurements described in

the preceding sections were taken into account when designing the MVN instrument. The main components of the instrument that should provide an accurate CXB measurement in the energy range 6-70 keV are:

1. A periodic aperture blocking system de- signed to continuously monitor the internal detector background and realized in the form of a rotating wheel that blocks the apertures of half the detectors by the same three-layer material of which the passive shield of the detector and the collimators themselves are composed at each instant of time. The wheel rotation period is 60 s, which should provide insignificant variations in the instrumental background of the detectors over one aperture modulation period.

2. A 100-μm-thick beryllium window of the detector that allows the charged particles with energies in the instruments operating range (6-70) to be cut off.

3. A system of calibration sources for each detector. The calibration sources (^{241}Am) can be inserted into the collimator on the instruments command to systematically monitor the instruments characteristics, its energy scale, and efficiency. During the planned scientific observations, the calibration sources are removed from the detectors field of view behind the collimator opaque to their photons.

4. A detector thermal stabilization unit. Its objective is to provide a constant detector temperature, which is very difficult to achieve for an instrument mounted at the external working place of the ISS due to the large heat flux differences on its sunlit and unlit sides. The system consists of heat pipes, heaters, external radiators, and electrically cooled modules. The operating temperature of the detectors is -30°C. The thermal stabilization unit is designed so as to provide a constant temperature of the detector crystals within 0.5 deg, which is very important for maintaining the instruments energy scale in a maximally stable state $\delta E/E < 0.5\%$.

The MVN instrument is scheduled to operate onboard the ISS for at least three years. The expected fraction of the useful time for observations is 80for the remaining time, the instrument will spend in the region of the South Magnetic Anomaly and high geomagnetic latitudes, in which a very high back- ground count rate of charged particles in the detector is expected.

At such a fraction of the useful time for observations and for an expected background count rate of charged particles $5 \times 10^{-3} - 5 \times 10^{-2}$ counts s^{-1} cm^{-2} keV^{-1} , the CXB signal will be recorded with a significance of 4-6σ in a day, 35- 55σ in 72 days (the ISS orbital precession period), and 80-120σ in a year.

The CXB detection significance will decrease with increasing energy due to the falling flux of CXB photons at a nearly constant (in units of count s-1 cm^{-2} keV^{-1}) background count rate of events related to the passage of charged particles. A more detailed prediction of the expected CXB detection significance over the entire planned onboard operation of the experiment is presented in Fig. 17.

Over three years of observations, MVN must obtain the CXB surface brightness spectrum in a wide energy range, 6-70 keV, with a record accuracy that, together with an accurate calibration of the detector energy scale and absolute efficiency and the collecting solid angle of the instrument, will specify a reference background surface brightness of the Universe for all observatories in this energy range.

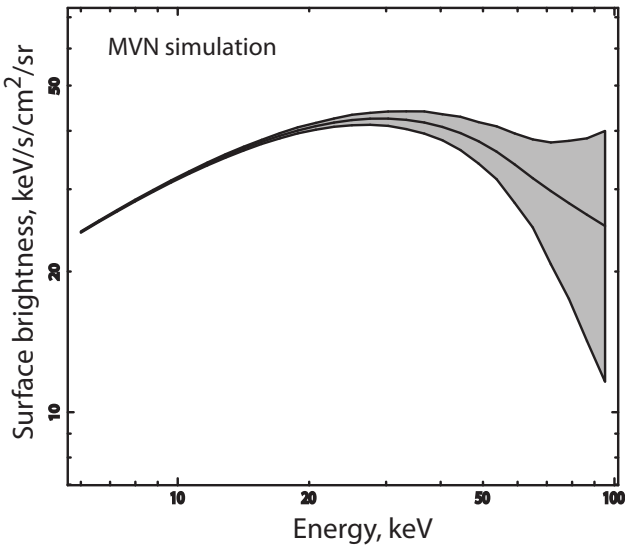

Fig. 17. CXB surface brightness spectrum expected from the operation of the MVN experiment over three years of observations. The gray region indicates the range of expected uncertainties in the surface brightness.

8. CONCLUSION

The cosmic X-ray background is one of the fundamental phenomena in X-ray astronomy. The fact that the CXB emission is the sum of the contributions from a large number of discrete sources, mostly the accreting supermassive black holes in the centers of galaxies at various distances from us (with a minor contribution

of the emission from ordinary galaxies and galaxy clusters, especially at energies below 2-5 keV), is currently believed to have been firmly established. This means that the CXB emission actually contains information about the history of accretion onto supermassive black holes over the entire lifetime of the visible Universe. Comparison of the spectral shape of the CXB surface brightness in the energy range 1-100 keV with the spectra of accreting supermassive black holes in the nearby Universe showed that the AGNs observed through the dust layer obscuring their emission in the standard X-ray (<10 keV), ultraviolet, and optical spectral ranges make a significant contribution to the CXB. Consequently, an accurate measurement of the CXB properties at energies above 2-10 keV makes it possible to correctly estimate the total mass accumulated in the black holes at the centers of galaxies.

The flux of X-ray photons from the sky is difficult to measure, because it is necessary to distinguish the events in the detectors related to the passage of X-ray photons from the events related to the passage of charged particles and their derivatives. The cosmic X-ray background is highly isotropic, which greatly complicates its reliable separation from the background of charged particles. The history of CXB measurements began in the 1960s, with the first experiments in X-ray astronomy. Different techniques and methodologies, most of which are presented in this paper, were used at different times to measure the CXB surface brightness in the energy range 1-100 keV.

The development of an experimental technique in the X-ray energy range and the advent of semiconductor detectors based on CdTe crystals have allowed an experiment whose objective would be the most accurate measurement of the CXB surface brightness in a wide energy range, 6-70 keV, to be proposed. Such an experiment is currently being developed at the Space Research Institute of the Russian Academy of Sciences and being prepared for its installation on the Russian segment of the International Space Station in the immediate future.

Author thanks M.N. Pavlinsky, A.A. Lutovinov, and N.P. Semena for their help in preparing the paper. The work was supported by RNF grant no. 14-12-01287

REFERENCES

1. Ajello, M., Greiner, J., Sato, G., et al. 2008, Astrophys. J., 689, 666
2. Barthelmy, S. D., Barbier, L. M., Cummings, J. R., et al. 2005, Space Science Reviews, 120, 143
3. Bautz, M. W., Pivovaroff, M. J., Kissel, S. E., et al. 2000, in Society of Photo-Optical Instrumentation Engineers (SPIE) Conference Series, Vol. 4012, X-Ray Optics, Instruments, and Missions III, ed. J. E. Truemper & B. Aschenbach, 53–67
4. Beuermann, K., Burwitz, V., & Rauch, T. 2007, in Astronomical Society of the Pacific Conference Series, Vol. 372, 15th European Workshop on White Dwarfs, ed. R. Napiwotzki & M. R. Burleigh, 221
5. Bleeker, J. A. M., & Deerenberg, A. J. M. 1970, Astrophys. J., 159, 215
6. Boldt, E. 1987, Physics Reports, 146, 215
7. Boldt, E. 1992, in The X-ray Background, ed. X. Barcons & A. C. Fabian, 115
8. Boldt, E. A., Desai, U. D., & Holt, S. S. 1969, Astrophys. J., 156, 427
9. Boldt, E. A., Desai, U. D., Holt, S. S., & Serlemitsos, P. J. 1970, in IAU Symposium, Vol. 37, Non-Solar X- and Gamma-Ray Astronomy, ed. L. Gratton, 309
10. Böttcher, M. 2007, Ap&SS, 309, 95
11. Churazov, E., Sazonov, S., Sunyaev, R., & Revnivtsev, M. 2008, MNRAS, 385, 719
12. Churazov, E., Sunyaev, R., Revnivtsev, M., et al. 2007, Astron. Astrophys., 467, 529
13. de Chambure, D., Laine, R., van Katwijk, K., et al. 1999, in Society of Photo-Optical Instrumentation Engineers (SPIE) Conference Series, Vol. 3737, Design and Engineering of Optical Systems II, ed. F. Merkle, 396–408
14. Dennerl, K., Briel, U. G., Freyberg, M. J., et al. 2002, ArXiv Astrophysics e-prints, astro-ph/0204242
15. Dennis, B. R., Suri, A. N., & Frost, K. J. 1973, Astrophys. J., 186, 97
16. Dumas, A., Horstman, H., & Horstman-Moretti, E. 1972, Ap&SS, 19, 495
17. Fabian, A. C., & Iwasawa, K. 1999, MNRAS, 303, L34
18. Farnik, F., Valnicek, B., Sylwester, B., Sylwester, J., & Jakimiec, J. 1984, Bulletin of the Astronomical Institutes of Czechoslovakia, 35, 158
19. Felten, J. E., & Morrison, P. 1966, Astrophys. J., 146, 686
20. Fukada, Y., Hayakawa, S., Ikeda, M., et al. 1975, Ap&SS, 32, L1
21. Gendreau, K. C., Mushotzky, R., Fabian, A. C., et al. 1995, PASJ, 47, L5
22. Giacconi, R., Gursky, H., Paolini, F. R., & Rossi, B. B. 1962, Physical Review Letters, 9, 439
23. Giacconi, R., & Rossi, B. 1960, Journal of Geophysical Research, 65, 773
24. Giacconi, R., Bechtold, J., Branduardi, G., et al. 1979, Astrophys. J. (Letters), 234, L1
25. Gilli, R. 2013, Memorie della Societa Astronomica Italiana, 84, 647
26. Gilli, R., Comastri, A., & Hasinger, G. 2007, Astron. Astrophys., 463, 79
27. Godet, O., Beardmore, A. P., Abbey, A. F., et al. 2009, Astron. Astrophys., 494, 775

28. Golenetskii, S. V., Mazets, E. P., Il'inskii, V. N., et al. 1971, Astrophysical Letters, 9, 69
29. Gorenstein, P., Kellogg, E. M., & Gursky, H. 1969, Astrophys. J., 156, 315
30. Gorenstein, P., & Mickiewicz, S. 1968, Review of Scientific Instruments, 39, 816
31. Grant, C. E., LaMarr, B., Miller, E., & Bautz, M. 2012, in American Institute of Physics Conference Series, Vol. 1427, American Institute of Physics Conference Series, ed. R. Petre, K. Mitsuda, & L. Angelini, 249–250
32. Harrison, F. A., Craig, W. W., Christensen, F. E., et al. 2013, Astrophys. J., 770, 103
33. Hayashida, K., Inoue, H., Koyama, K., Awaki, H., & Takano, S. 1989, PASJ, 41, 373
34. Hickox, R. C., & Markevitch, M. 2006, Astrophys. J., 645, 95
35. —. 2007, Astrophys. J. (Letters), 661, L117
36. Horstman, H. M., Cavallo, G., & Moretti-Horstman, E. 1975, Nuovo Cimento Rivista Serie, 5, 255
37. Ishida, M., Tsujimoto, M., Kohmura, T., et al. 2011, PASJ, 63, 657
38. Jahoda, K., Markwardt, C. B., Radeva, Y., et al. 2006, Astrophys. J. Suppl. Ser., 163, 401
39. Jahoda, K., Mushotzky, R. F., Boldt, E., & Lahav, O. 1991, Astrophys. J. (Letters), 378, L37
40. Jung, G. V. 1989, Astrophys. J., 338, 972
41. Katayama, H., Takahashi, I., Ikebe, Y., Matsushita, K., & Freyberg, M. J. 2004, Astron. Astrophys., 414, 767
42. Kinzer, R. L., Johnson, W. N., & Kurfess, J. D. 1978, Astrophys. J., 222, 370
43. Kinzer, R. L., Jung, G. V., Gruber, D. E., Matteson, J. L., & Peterson, L. E. 1997, Astrophys. J., 475, 361
44. Kirsch, M. G., Briel, U. G., Burrows, D., et al. 2005, in Society of Photo-Optical Instrumentation Engineers (SPIE) Conference Series, Vol. 5898, UV, X-Ray, and Gamma-Ray Space Instrumentation for Astronomy XIV, ed. O. H. W. Siegmund, 22–33
45. Krumrey, M. K., Scholze, F., & Ulm, G. 2004, in Society of Photo-Optical Instrumentation Engineers (SPIE) Conference Series, Vol. 5501, High-Energy Detectors in Astronomy, ed. A. D. Holland, 277–285
46. Makino, F. 1975, Ap&SS, 37, 115
47. Malaguti, G., Bazzano, A., Bird, A. J., et al. 2003, Astron. Astrophys., 411, L173
48. Mandelshtam, S. L., & Efremov, A. I. 1957, Physics-Uspekhi, 63, 163
49. Mandel'Shtam, S. L., & Tindo, I. P. 1967, ZhETF Pisma Redaktsiiu, 6, 796
50. Markevitch, M., Bautz, M. W., Biller, B., et al. 2003, Astrophys. J., 583, 70
51. Marshall, F. E., Boldt, E. A., Holt, S. S., et al. 1980, Astrophys. J., 235, 4
52. Mather, J. C., Cheng, E. S., Cottingham, D. A., et al. 1994, Astrophys. J., 420, 439
53. Matsuoka, M., Oda, M., Ogawara, Y., Hayakawa, S., & Kato, T. 1969, Ap&SS, 4, 44
54. Mazets, E. P., Golenetskii, S. V., Ilinskii, V. N., Gurian, I. A., & Kharitonova, T. V. 1975, Ap&SS, 33, 347
55. McCammon, D., & Sanders, W. T. 1990, Ann. Rev. of Astron. and Astrophys., 28, 657
56. Miyaji, T., Lahav, O., Jahoda, K., & Boldt, E. 1994, Astrophys. J., 434, 424
57. Moretti, A., Campana, S., Lazzati, D., & Tagliaferri, G. 2003, Astrophys. J., 588, 696
58. Moretti, A., Pagani, C., Cusumano, G., et al. 2009, Astron. Astrophys., 493, 501
59. Parmar, A. N., Oosterbroek, T., Orr, A., et al. 1999, Astron. Astrophys. Suppl. Ser., 136, 407
60. Petry, D. 2005, in American Institute of Physics Conference Series, Vol. 745, High Energy Gamma-Ray Astronomy, ed. F. A. Aharonian, H. J. Völk, & D. Horns, 709–714
61. Plucinsky, P. P., Schulz, N. S., Marshall, H. L., et al. 2003, in Society of Photo-Optical Instrumentation Engineers (SPIE) Conference Series, Vol. 4851, X-Ray and Gamma-Ray Telescopes and Instruments for Astronomy., ed. J. E. Truemper & H. D. Tananbaum, 89–100
62. Pravdo, S. H. 1976, PhD thesis, National Aeronautics and Space Administration. Goddard Space Flight Center, Greenbelt, MD.
63. Prigozhin, G. Y., Bautz, M. W., & Ricker, Jr., G. R. 2003, in Society of Photo-Optical Instrumentation Engineers (SPIE) Conference Series, Vol. 4851, X-Ray and Gamma-Ray Telescopes and Instruments for Astronomy., ed. J. E. Truemper & H. D. Tananbaum, 149–156
64. Prigozhin, G. Y., Kissel, S. E., Bautz, M. W., et al. 2000, in Society of Photo-Optical Instrumentation Engineers (SPIE) Conference Series, Vol. 4012, X-Ray Optics, Instruments, and Missions III, ed. J. E. Truemper & B. Aschenbach, 720–730
65. Puskin, J. S. 1970, SAO Special Report, 318
66. Revnivtsev, M., Gilfanov, M., Jahoda, K., & Sunyaev, R. 2005, Astron. Astrophys., 444, 381
67. Revnivtsev, M., Gilfanov, M., Sunyaev, R., Jahoda, K., & Markwardt, C. 2003, Astron. Astrophys., 411, 329
68. Revnivtsev, M., Molkov, S., & Sazonov, S. 2008, Astron. Astrophys., 483, 425
69. Revnivtsev, M., Semena, N., Akimov, V., et al. 2012, in Society of Photo-Optical Instrumentation Engineers (SPIE) Conference Series, Vol. 8443, Society of Photo-Optical Instrumentation Engineers (SPIE) Conference Series
70. Rothschild, R., Boldt, E., Holt, S., et al. 1979, Space Science Instrumentation, 4, 269
71. Sazonov, S., Churazov, E., Sunyaev, R., & Revnivtsev, M. 2007, MNRAS, 377, 1726
72. Sazonov, S., Krivonos, R., Revnivtsev, M., Churazov, E., & Sunyaev, R. 2008, Astron. Astrophys., 482, 517
73. Scharf, C. A., Jahoda, K., Treyer, M., et al. 2000, Astrophys. J., 544, 49

74. Schwartz, D. A. 1970, Astrophys. J., 162, 439
75. Schwartz, D. A., Murray, S. S., & Gursky, H. 1976, Astrophys. J., 204, 315
76. Schwartz, D. A., & Peterson, L. E. 1974, Astrophys. J., 190, 297
77. Setti, G., & Woltjer, L. 1989, Astron. Astrophys., 224, L21
78. Seward, F., Chodil, G., Mark, H., Swift, C., & Toor, A. 1967, Astrophys. J., 150, 845
79. Seward, F. D., Grader, R. J., Toor, A., Burginyon, G. A., & Hill, R. W. 1974, in Electron Contamination in X-ray Astronomy Experiments, ed. S. S. Holt
80. Silk, J. 1970, Space Science Reviews, 11, 671
81. Skelton, R. T., Matteson, J. L., Slassi-Sennou, S. A., et al. 2000, in American Institute of Physics Conference Series, Vol. 510, American Institute of Physics Conference Series, ed. M. L. McConnell & J. M. Ryan, 712–716
82. Soltan, A. 1982, MNRAS, 200, 115
83. Sunyaev, R. A., & Zeldovich, Y. B. 1970, Ap&SS, 7, 3
84. Syunyaev, R. A., Borozdin, K. N., Aleksandrovich, N. L., et al. 1994, Astronomy Letters, 20, 777
85. Tanaka, Y., & Bleeker, J. A. M. 1977, Space Science Reviews, 20, 815
86. Terrier, R., Lebrun, F., Bazzano, A., et al. 2003, Astron. Astrophys., 411, L167
87. Toor, A., & Seward, F. D. 1974, Astron. J., 79, 995
88. Tsujimoto, M., Guainazzi, M., Plucinsky, P. P., et al. 2011, Astron. Astrophys., 525, A25
89. Ueda, Y., Akiyama, M., Hasinger, G., Miyaji, T., & Watson, M. G. 2014, Astrophys. J., 786, 104
90. Urry, C. M., & Padovani, P. 1995, PASP, 107, 803
91. Vette, J. I. 1962, Journal of Geophysical Research, 67, 1731
92. Warwick, R. S., Pye, J. P., & Fabian, A. C. 1980, MNRAS, 190, 243
93. Wik, D. R., Hornstrup, A., Molendi, S., et al. 2014, ArXiv e-prints, arXiv:1403.2722
94. Wilson-Hodge, C. A., Cherry, M. L., Case, G. L., et al. 2011, Astrophys. J. (Letters), 727, L40
95. Wright, E. L., Mather, J. C., Fixsen, D. J., et al. 1994, Astrophys. J., 420, 450

Translated by V. Astakhov for Astronomy Letters